Phase Transitions Mechanism and Distortion of $SbCl_6^{3-}$ Octahedra in Bis(*n*-butylammonium) Pentachloroantimonate(III) $(C_4H_9NH_3)_2[SbCl_5]$

Bartosz Zarychta and Jacek Zaleski

Institute of Chemistry, University of Opole, Oleska 48, 45-052 Opole, Poland

Reprint requests to Prof. J. Zaleski. Fax: (0048)-77-4410741. E-mail: zaleski@uni.opole.pl

Z. Naturforsch. **61b,** 1101 – 1109 (2006); received February 1, 2006

Bis(*n*-butylammonium) pentachloroantimonate(III) was obtained in a reaction of *n*-butylammonium chloride and antimony trichloride (molar ratio 2 : 1; cation : Sb) in acidic aqueous solution. To obtain further information about the mechanism of the earlier reported phase transitions at 229 and 315 K the structure was determined at 100, 260 and 340 K. The orthorhombic system was found in all phases, space groups *Ibam* at 340 K and *Pccn* at 260 and 100 K. In all phases the anionic sublattice consists of $[SbCl_6]^{3-}$ octahedra, connected *via cis* chlorine atoms, forming one-dimensional zig-zag $\{[SbCl_5]^{2-}\}_n$ chains extended along the *c* direction. The *n*-butylammonium cations are located between the inorganic chains, with $-NH_3^+$ groups facing the oppositely charged polyanions. The phase transitions are of the order-disorder type. They are related to changes in molecular dynamics of the *n*-butylammonium cations. At high temperature the cations reorient, on decreasing temperature the reorientations are successfully frozen. This leads to the formation on N-H…Cl hydrogen bonds, which significantly deform the octahedral coordination of the Sb atoms.

Key words: Chloroantimonates(III), *n*-Butylammonium Cation, Phase Transition, Disorder

Introduction

Alkylammonium halogenoantimonates(III) and bismuthates(III) of the general formula $R_aM_bX_{3b+a}$ (where R is an organic cation; M is Sb or Bi and X is Cl, Br or I) are very interesting groups due to the polar properties of a number of compounds [1 – 3]. The most interesting from the point of view of physical properties and technical applications are compounds with relatively small cations. They typically show a sequence of phase transitions, caused by changes in rotational motions of cations, which take place on changing temperature [4 – 6].

On decreasing temperature, the rotations of molecules or ions in the solid state are usually frozen. This leads to the presence of one or more phase transitions. Typically the mechanisms of phase transitions are complex, because the dynamics of both sublattices may be involved. The compounds are molecular-ionic salts, with anionic sublattices composed of deformed MX_6^{3-} octahedra or MX_5^{2-} square pyramids, which may be isolated or connected with each other by corners, edges or faces, forming various structural geometries [3, 7].

The geometry of the anionic sublattice typically depends on size, shape and charge of cations. Cations are placed in the voids of an anionic sublattice. At high temperatures, small cations typically reorient in the solid state. On lowering temperature the reorientations of cations are slowing down and finally are frozen at low temperature, which leads to the formation of N–H…X hydrogen bonding networks [8 – 10].

In the compounds, bismuth(III) and antimony(III) centres possess a lone electron pair. In case of a lack of external interactions it is not stereochemically active, since it occupies an *s*-orbital of spherical symmetry. It should be mentioned, however, that the presence of a lone pair increases Sb-X bond length. The typical Sb^V-Cl bond length in $SbCl_6^-$ is 2.382(5) Å. It is almost the same in all determined structures. Large differences are, however, seen in the octahedral geometry $SbCl_6^{3-}$, where Sb^{III}-Cl bond length is significantly longer 2.647(1) Å [10]. The lone electron pair may be easily deformed from the initial symmetry as a result of a formation of M–X–M (M = Bi, or Sb; X = Cl, Br or I) bonds. When two octahedra are joined together having common (X) halogen atoms the bridging M-X bond length is increased, whereas the oppo-

	340 K	260 K	100 K
Empirical formula		$(C_4H_9NH_3)_2[SbCl_5]$	
Formula weight		447.29	
Crystal colour		colourless	
Crystal size [mm^3]	$0.2\times0.2\times0.15$	$0.15\times0.15\times0.1$	
Crystal system		orthorhombic	
Space group	*Ibam*	*Pccn*	
Unit cell dimensions [Å, °]	$a = 18.218(1)$	$a = 18.120(1)$	$a = 18.323(1)$
	$b = 26.715(2)$	$b = 26.996(2)$	$b = 27.911(2)$
	$c = 7.924(1)$	$c = 7.789(1)$	$c = 7.377(1)$
Volume [Å^3]	3856.7(4)	3810.0(4)	3772.7(4)
Z	8	8	8
Density (calculated) [g·cm^{-3}]	1.541	1.560	1.575
Wavelength [Å]		0.071073	
Absorption coefficient [mm^{-1}]	2.107	2.133	2.154
$F(000)$		1776	
θ Range [°]	3.19 – 25	2.95 – 25	3.32 – 25
Index ranges	$-21 \le h \le 21$;	$-21 \le h \le 24\backslash 1$;	$-21 \le h \le 21$;
	$-31 \le k \le 31$;	$-31 \le k \le 32$;	$-33 \le k \le 33$;
	$-9 \le l \le 6$	$-9 \le l \le 6$	$-5 \le l \le 8$
Reflections collected/unique	11413/1829	21660/3340	21200/3303
Observed reflections $[I > 2\sigma(I)]$	1303	2200	3144
Data/parameters	1829/121	3340/155	3303/146
Goodness of fit on F^2	1.176	1.120	1.270
Final R indices $[I > 2\sigma(I)]$	$R_1 = 0.0467$,	$R_1 = 0.0495$,	$R_1 = 0.0519$,
	$wR_2 = 0.1336$	$wR_2 = 0.0884$	$wR_2 = 0.1158$
R Indices (all data)	$R_1 = 0.0677$,	$R_1 = 0.0969$,	$R_1 = 0.0541$,
	$wR_2 = 0.1459$	$wR_2 = 0.1042$	$wR_2 = 0.1168$
Largest diff. peak and hole [e·Å^{-3}]	0.61 and −0.45	0.55 and −0.38	0.94 and −1.31

Table 1. The crystal data, X-ray measurements and structure determination summary for $(C_4H_9NH_3)_2[SbCl_5]$ at 340, 260 and 100 K.

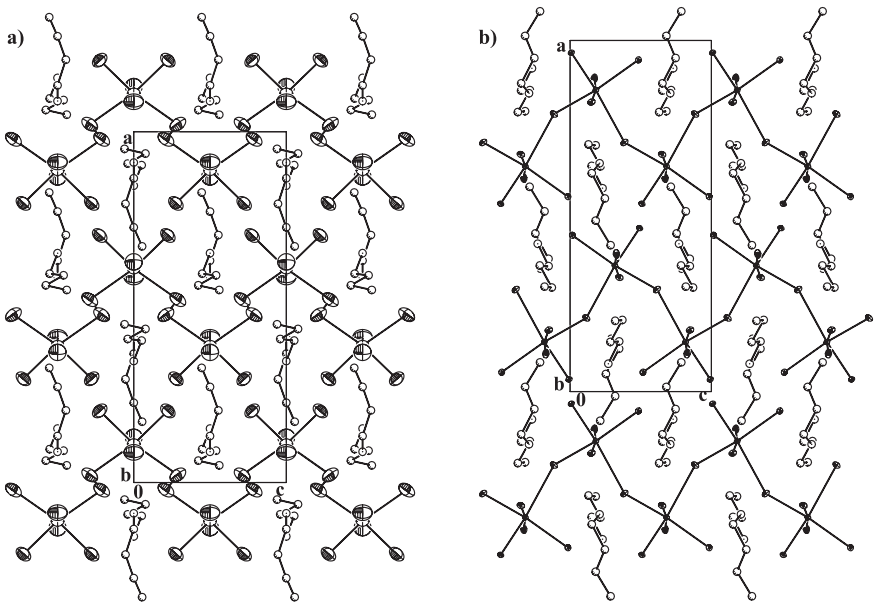

Fig. 1. Packing diagram of the $(C_4H_9NH_3)_2[SbCl_5]$ crystal at a) 340 K; and b) 100 K. Displacement ellipsoids are plotted at the 25% probability level. The second positions of disordered atoms are not shown for clarity.

site, terminal one, is decreased. As an example we may take the structure of $[C(NH_2)_3]_3[Sb_2Cl_9]$, where in the octahedral configuration of the antimony atom there are three bridging Sb-Cl bonds, the length of which is 2.915(10) Å, whereas the three terminal ones, have a length of 2.446(1) Å [11]. It should be noted that the increase of bond lengths compared to not deformed octahedron in this case is 0.27 Å, whereas the decrease in length of the opposite bonds is 0.20 Å. The changes in geometry are the result of the change of the position

of the lone electron pair, in comparison to a situation without a deformation of the octahedral coordination [12, 13].

Alkylammonium chloroantimonates(III) are generally obtained by mixing the chosen alkylammonium chloride with antimony trichloride or antimony(III) oxide changing the molar ratio of reagents in an aqueous solution of hydrochloric acid.

This paper is a part of a larger project devoted to the syntheses, crystal structures, phase transitions and molecular motions of halogenoantimonates(III) and bismuthates(III).

Recently, DSC measurements of the title compound have been reported [6]. The DSC plots between 150 and 340 K for $(n\text{-}C_4H_9NH_3)_2[SbCl_5]$ recorded on heating and cooling runs have disclosed two distinct thermal anomalies at 229 and 315 K (temperatures on heating). The former peak is quite sharp, exhibiting a c_p 'tail' stretching back to 190 K, whereas the latter is broad with a peak temperature of about 315 K. The temperatures, enthalpies and entropies of the transitions are: $T_1 = 229$ K, $\Delta H_1 = 1.79\ \mathrm{kJ \cdot mol^{-1}}$, $\Delta S_1 = 7.5\ \mathrm{J \cdot mol^{-1} \cdot K^{-1}}$ (mixed first and second order phase transition) and $T_2 = 315$ K, $\Delta H_2 = 0.36\ \mathrm{kJ \cdot mol^{-1}}$, $\Delta S_1 = 7.5\ \mathrm{J \cdot mol^{-1} \cdot K^{-1}}$ (second order).

In order to obtain further information about the mechanisms of phase transitions as well as on the effect of interactions between organic and inorganic sublattices, we have determined the crystal structures of $(n\text{-}C_4H_9NH_3)_2[SbCl_5]$ between 100 K and 340 K.

Results and Discussion

X-ray diffraction studies

X-ray single-crystal diffraction studies have been undertaken to obtain further information about the structural changes in the phase transitions reported earlier at 315 and 229 K [6]. The X-ray investigations have been performed at 340, 260 and 100 K.

In all phases the crystals are orthorhombic. At 100 K as well as at 260 K the space group is *Pccn*, whereas at 340 K it is *Ibam*. At all temperatures, the structures are composed of infinite one-dimensional $[\{SbCl_5\}^{2-}]_n$ chains composed of $[SbCl_6]^{3-}$ octahedra, sharing two *cis* corners with two neighbouring entities. The cations attracted to the anionic sublattice by N–H...Cl hydrogen bonds are located between the inorganic chains. The crystal packing is depicted in Fig. 1. Such polyanionic, one-dimensional zig-zag chains are most com-

Table 2. Atomic coordinates $(\cdot 10^4)$ and equivalent isotropic displacement parameters $(\mathrm{Å}^2 \cdot 10^3)$ for non-hydrogen atoms of $(C_4H_9NH_3)_2[SbCl_5]$ at 340, 260 and 100 K.

Atom	*x*	*y*	*z*	U_{eq} [a]
		340 K		
Sb1	3903(1)	1830(1)	5000	85(1)
Cl1	4785(2)	1919(2)	7890(7)	147(2)
Cl2	2957(1)	1762(1)	2763(3)	131(1)
Cl3	4140(2)	760(1)	5000	167(1)
Cl4	3711(2)	2743(1)	5000	139(1)
N1	1538(6)	2341(4)	5000	168(4)
C1	95(1)	197(1)	448(4)	18(1)
C2	91(2)	155(1)	540(7)	24(1)
C3	62(2)	116(1)	423(4)	28(1)
C4	49(2)	77(1)	560(5)	30(1)
N2	588(1)	815(1)	5000	36(2)
C5	633(1)	570(9)	5000	216(8)
C6	706(2)	50(1)	554(6)	26(1)
C7	772(3)	49(3)	5000	29(1)
C7A	746(3)	62(4)	5000	29(2)
C8	827(2)	46(1)	445(7)	31(2)
		260 K		
Sb1	1399(1)	−690(1)	2067(1)	59(1)
Cl1	344(1)	−800(1)	221(2)	88(1)
Cl2	540(1)	−706(1)	4699(2)	85(1)
Cl2A	1620(1)	−1745(1)	2159(3)	118(1)
Cl3	1232(1)	218(1)	1919(2)	94(1)
Cl4	−912(3)	−162(2)	253(1)	90(2)
N1	−1484(6)	−45(1)	330(1)	130(3)
C1	−1552(8)	−96(1)	267(2)	21(1)
C2	−201(1)	−128(1)	339(2)	25(1)
C3	−193(1)	−181(1)	286(3)	35(1)
C4	340(1)	−1600(4)	173(2)	22(1)
N2	372(1)	−194(1)	226(2)	20(1)
C5	455(1)	−193(1)	210(2)	22(1)
C6	493(2)	−212(1)	316(3)	20(1)
C7	532(4)	−184(2)	225(5)	19(1)
C7A	583(1)	−202(1)	309(2)	30(1)
C8	2815(1)	−631(1)	4160(2)	104(1)
		100 K		
Sb1	1413(1)	−709(1)	1828(1)	19(1)
Cl1	2906(1)	−579(1)	3849(2)	28(1)
Cl2	346(1)	−898(1)	80(2)	26(1)
Cl2A	551(1)	−766(1)	4842(2)	23(1)
Cl3	1752(1)	−1678(1)	1511(2)	26(1)
Cl4	1080(1)	169(1)	1719(2)	30(1)
N1	−792(3)	−191(2)	2705(8)	25(1)
C1	−1427(4)	−466(3)	3472(9)	26(2)
C2	−1412(4)	−985(3)	2849(9)	26(2)
C3	−2038(4)	−1269(3)	3701(11)	34(2)
C4	−2014(5)	−1799(3)	3189(14)	47(2)
N2	3498(3)	−1589(2)	2089(7)	19(1)
C5	3781(4)	−2063(3)	1533(11)	32(2)
C6	4501(4)	−2181(3)	2463(11)	34(2)
C7	5131(4)	−1885(3)	1812(12)	38(2)
C8	5832(5)	−1994(4)	2868(18)	74(4)

[a] U_{eq} is defined as one third of the trace of the orthogonalized U_{ij} tensor.

340 K		260 K		100 K	
Sb1-Cl1^{II}	2.928(5)	Sb1-Cl1	3.046(2)	Sb1-Cl1	3.136(2)
Sb1-Cl1^{I}	2.808(6)	Sb1-Cl1^{III}	2.679(2)	Sb1-Cl1^{III}	2.553(2)
Sb1-Cl2	2.478(2)	Sb1-Cl2	2.410(2)	Sb1-Cl2	2.400(2)
		Sb1-Cl2A	2.575(2)	Sb1-Cl2A	2.733(2)
Sb1-Cl3^{I}	2.893(4)	Sb1-Cl3	2.877(2)	Sb1-Cl3	2.784(2)
Sb1-Cl4	2.463(3)	Sb1-Cl4	2.472(2)	Sb1-Cl4	2.527(2)
N(1)-C(1)	1.51(3)	N1-C1	1.435(11)	N1-C1	1.504(9)
C(1)-C(2)	1.34(4)	C1-C2	1.469(17)	C1-C2	1.521(10)
C(2)-C(3)	1.48(4)	C2-C3	1.324(17)	C2-C3	1.530(10)
C(3)-C(4)	1.54(4)	C3-C4	1.489(18)	C3-C4	1.527(11)
N(2)-C(5)	1.04(2)	N2-C5	1.158(12)	N2-C5	1.480(9)
C(5)-C(6)	1.41(3)	C5-C6	1.51(2)	C5-C6	1.523(11)
C(6)-C(7)	1.29(6)	C6-C7	1.19(2)	C6-C7	1.500(11)
C(7)-C(8)	1.08(5)	C7-C8	1.66(3)	C7-C8	1.532(12)
N(1)-C(1)-C(2)-C(3)	−151(2)	N(1)-C(1)-C(2)-C(3)	173.9(13)	N(1)-C(1)-C(2)-C(3)	177.4(6)
C(1)-C(2)-C(3)-C(4)	−170(3)	C(1)-C(2)-C(3)-C(4)	−168.9(15)	C(1)-C(2)-C(3)-C(4)	−176.7(7)
N(2)-C(5)-C(6)-C(7)	−108(8)	N(2)-C(5)-C(6)-C(7)	147.8(18)	N(2)-C(5)-C(6)-C(7)	−70.4(9)
C(5)-C(6)-C(7)-C(8)	−142(6)	C(5)-C(6)-C(7)-C(8)	−169.8(16)	C(5)-C(6)-C(7)-C(8)	176.4(8)
Cl1-Sb1-Cl1^{I}	109.30(19)	Cl1^{III}-Sb1-Cl1	90.07(2)	Cl1^{III}-Sb1-Cl1	88.09(2)
Cl1^{I}-Sb1-Cl1^{II}	89.51(4)				
Cl1^{I}-Sb1-Cl3	89.89(11)	Cl1^{III}-Sb1-Cl3	90.33(7)	Cl1^{III}-Sb1-Cl3	87.55(5)
Cl2-Sb1-Cl1^{I}	79.66(11)	Cl2-Sb1-Cl1^{III}	85.68(6)	Cl2-Sb1-Cl1^{III}	88.12(6)
Cl2-Sb1-Cl2^{I}	91.33(12)	Cl2-Sb1-Cl2A	89.70(6)	Cl2-Sb1-Cl2A	87.32(5)
Cl2-Sb1-Cl3	91.75(7)	Cl2-Sb1-Cl3	90.20(7)	Cl2-Sb1-Cl3	85.60(6)
Cl2-Sb1-Cl4	88.56(7)	Cl2-Sb1-Cl4	89.83(7)	Cl2-Sb1-Cl4	89.92(6)
Cl2^{I}-Sb1-Cl1^{II}	99.51(11)	Cl2A-Sb1-Cl1	94.77(6)	Cl2A-Sb1-Cl1	97.12(5)
Cl2^{I}-Sb1-Cl3	91.75(7)	Cl2A-Sb1-Cl3	92.75(7)	Cl2A-Sb1-Cl3	98.09(5)
Cl3-Sb1-Cl1	89.89(11)	Cl3-Sb1-Cl1	85.45(6)	Cl3-Sb1-Cl1	87.60(5)
Cl4-Sb1-Cl1	89.85(10)	Cl4-Sb1-Cl1	94.41(6)	Cl4-Sb1-Cl1	96.54(6)
Cl4-Sb1-Cl1^{I}	89.85(11)	Cl4-Sb1-Cl1^{III}	88.12(7)	Cl4-Sb1-Cl1^{III}	87.31(6)
Cl4-Sb1-Cl2^{I}	88.56(7)	Cl4-Sb1-Cl2A	88.81(6)	Cl4-Sb1-Cl2A	86.67(6)
Cl1I-Sb1-Cl2^{I}	170.89(10)	Cl1^{III}–Sb1- Cl2A	174.45(6)	Cl1^{III}-Sb1-Cl2A	172.45(6)
Cl2-Sb1-Cl1	170.89(10)	Cl2-Sb1-Cl1	173.90(6)	Cl2-Sb1-Cl1	172.35(5)
Cl2-Sb1-Cl1^{II}	169.16(12)				
Cl4-Sb1-Cl3	179.55(11)	Cl4-Sb1-Cl3	178.44(7)	Cl4-Sb1-Cl3	173.29(6)
Sb1-Cl1-Sb1^{IV}	158(1)	Sb1-Cl1-Sb1^{V}	153.8(8)	Sb1-Cl1-Sb1^{V}	145.0(2)

Table 3. The comparison of selected bond lengths (Å) and angles (°) for $(C_4H_9NH_3)_2[SbCl_5]$ at 340, 260 and 100 K. Symmetry codes: ^{I} x, y, $2-z$; ^{II} $-x+2$, y, $5/2-z$; ^{III} $-x+3/2$, y, $-1/2+z$; ^{IV} $1-x$, y, $1/2+z$; ^{V} $1/2-x$, $-y$, $-1/2+z$.

Table 4. The hydrogen bond geometries (Å, °) for $(C_4H_9NH_3)_2[SbCl_5]$ at 340 K, 260 K and 100 K. Symmetry codes: ^{I} $-x+3/2$, y, $z-1/2$, ^{II} $-x+3/2$, y, $z+1/2$, ^{III} $-x+1$, $-y+2$, $-z+1$, ^{IV} $-x+1$, $-y+2$, $-z$; ^{V} $-x$, $-y$, $1-z$.

D–H···A	D–H	H···A	D···A	D–H···A
		340 K		
N2-H2A···Cl3	0.84	2.37	3.169(19)	157
		260 K		
N2-H2A···Cl3	0.90	2.36	3.258(11)	174
N1-H1A···Cl2A^{V}	0.90	2.45	3.254(6)	150
		100K		
N1-H1C···Cl2A	0.89	2.47	3.333(6)	164
N2-H2A···Cl3	0.89	2.47	3.237(5)	144
N2-H2B···Cl2A^{I}	0.89	2.49	3.326(6)	156
N2-H2C···Cl3^{II}	0.89	2.42	3.304(5)	174
N1-H1A···Cl2A^{III}	0.89	2.43	3.256(6)	154
N1-H1B···Cl4^{IV}	0.89	2.43	3.307(6)	170

mon for chloroantimonates(III) of the E_2SbCl_5 formula (E =monocation) [2].

The crystal data and the structure determination details for $(C_4H_9NH_3)_2[SbCl_5]$ at 100, 260 and 340 K are listed in Table 1. The final atomic coordinates and equivalent isotropic displacement parameters for non-H atoms in both phases are shown in Table 2. The bond lengths and angles are presented in Table 3 whereas the hydrogen bonding geometry is presented in Table 4.

Structure at 340 K

The octahedral coordination of the antimony atom is distorted. The infinite $[\{SbCl_5\}^{2-}]_n$ chain (Fig. 1) is extended along the *c* direction. Two chlorine atoms of the coordination sphere of each antimony atom are bridging and four are terminal. The bridging chlorine atoms are disordered with equal occupancy.

In the analogous structure of guanidinium hexachloroantimonate(III) $Gu_2[SbCl_5] \cdot GuCl$, (Gu = $[(NH_2)_3C]^+$) there is a characteristic pattern of bond

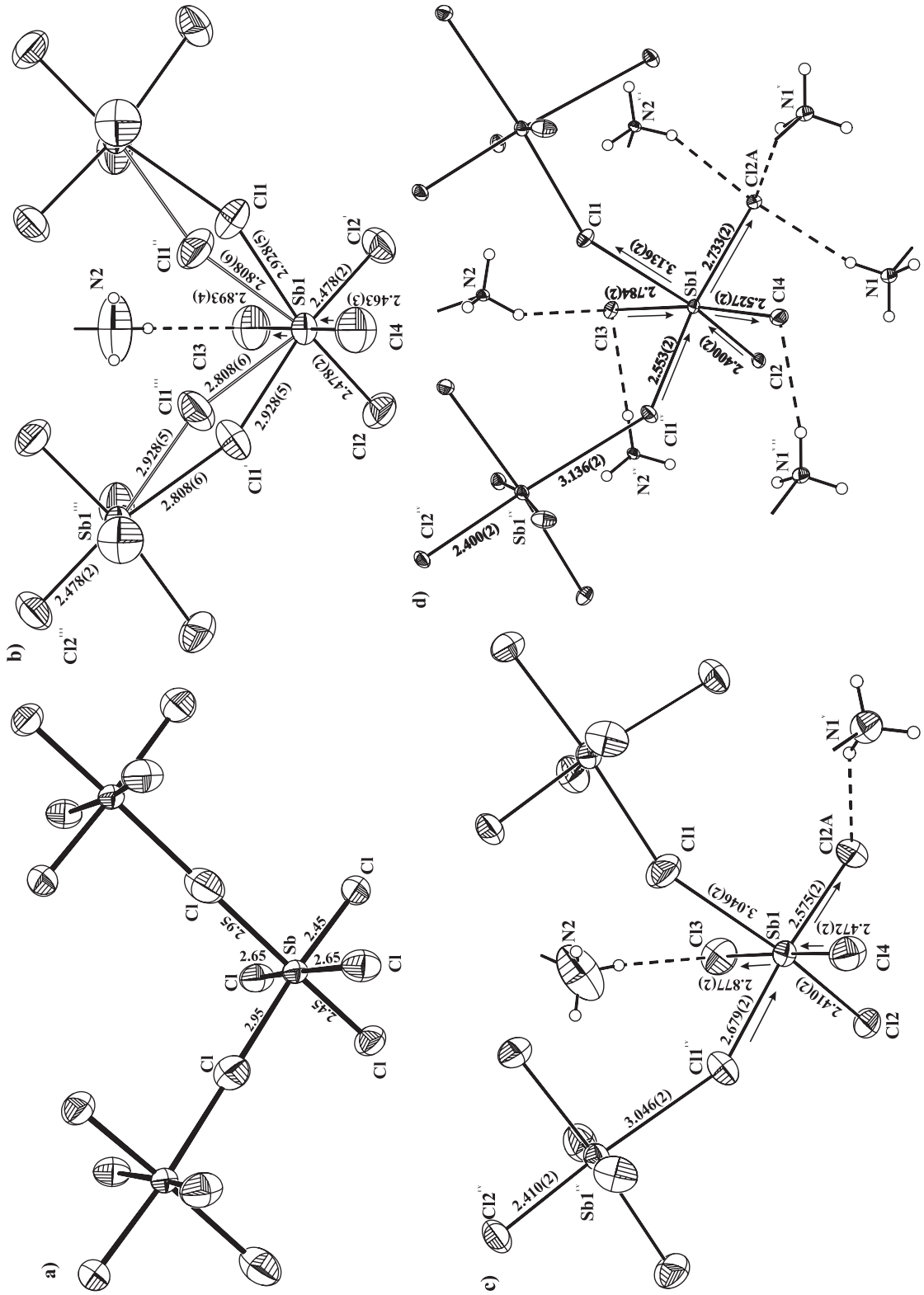

Fig. 2. The distortion of the polyanionic $(SbCl_5)^{2-}$ sublattice by N-H…Cl hydrogen bonds. a) The geometry of the undistorted $(SbCl_5)^{2-}$ part of the anionic sublattice; b), c), d) the geometry of $(C_4H_9NH_3)_2[SbCl_5]$ crystals at 340; 260; and 100 K, respectively. Displacement ellipsoids are plotted at the 25% probability level. The H and C atoms have been omitted for clarity. Symmetry codes: ^{I} $x, y, 1-z$; ^{II} $1-x, y, 3/2-z$; ^{III} $1-x, y, -1/2+z$; ^{IV} $1/2-x, y, -1/2+z$; ^{V} $-x, -y, 1-z$; ^{VI} $3/2-x, y, 1-z$; ^{VII} $1-x, 2-y, -z$.

lengths in the coordination sphere of the central antimony(III) atom. The longest Sb–Cl bonds involve bridging halogen atoms (2.900(7) Å) and the shortest are terminal ones, opposite to bridging (2.495(7) Å). Two other terminal Sb-X bonds have intermediate lengths and are distorted from the ideal geometry by N-H…Cl hydrogen bonds [14]. The geometry of the $(SbCl_5)^{2-}$ part of the anionic sublattice of $Gu_2[SbCl_5]\cdot GuCl$, is presented in Fig. 2a.

A similar situation we have in the present structure (see Fig. 2b). There are two sets of Sb-Cl bonds. One set comprises two pairs. Each pair possesses one bridging and one terminal Sb-Cl bond. They are located opposite. The second pair is composed of two terminal Sb-Cl bonds. The bond lengths of the first set are close to that found in $Gu_2[SbCl_5]\cdot GuCl$. The terminal bond length is 2.478(2), whereas the bridging one is split between two positions with Sb-Cl bond lengths of 2.808(6) and 2.928(5) Å. The second pair possesses two terminal bonds lying *trans* to each other. Generally in case of lack of interactions of those bonds with cations they should have the same length, roughly 2.65 Å. The Sb1-Cl3 bond is strongly extended to 2.893(4) Å, whereas the second one (Sb1-Cl4) is much shorter, 2.463(3) Å, being the shortest in the octahedral coordination of the Sb1 atom. Such a deformation should be attributed to the presence of a relatively strong hydrogen bond to Cl3 (N2-H2A…Cl3) (Table 4).The presence of this interaction and the lack of hydrogen bonds to Cl4 cause a significant increase of length of the Sb1-Cl3 bond and consequently, the decrease of length of the opposite one (Sb1-Cl4). This situation is related to a change in a position of the lone electron pair on Sb1, which is moved in the Cl3 direction.

The Cl-Sb-Cl angles involving chlorine atoms *cis* to each other range from 79.66(11) to 99.51(11)°, while those located *trans* are between 169.2(1) and 179.6(1)°. The angle Sb1-Cl1-$Sb1^{I}$ amounts to 157.9(2)°.

There are two crystallographically non-equivalent *n*-butylammonium cations $(C_4H_9NH_3)^+$ in the unit cell. They are located between the polyanionic chains and are disordered (Fig. 3a). The type of disorder is similar. In the N1 cation it is realized by the presence of two positions for all carbon atoms, whereas in the N2 cation, one carbon atom (connected to a nitrogen) remains not split. All split atoms have the occupation factor of 0.5. The geometrical parameters of the *n*-butylammonium cations are presented in Table 3. Be-

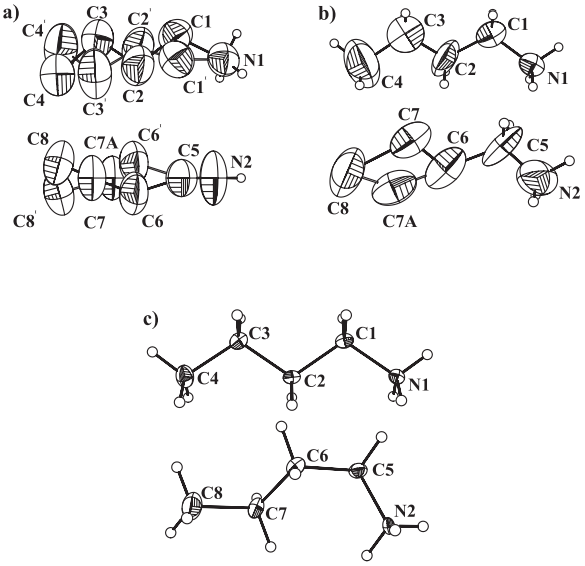

Fig. 3. The *n*-butylammonium cations in the structure of $(C_4H_9NH_3)_2[SbCl_5]$ at a) 340 K; b) 260 K; and c) 100 K. Displacement ellipsoids are plotted at the 25% probability level. Symmetry code: (^{I}) $x, y, 1-z$.

cause of the dynamical disorder, the precision in determination of atom positions is lower. The standard deviations of bond lengths and angles are higher in comparison to the data at lower temperatures. Since there is only one hydrogen bond N2-H2A…Cl3 (Table 4) present, it suggests that the N2 cation is more strongly bound to the anionic sublattice.

Structure at 260 K

Below the high-temperature phase transition at $T_{c1} = 315$ K the title salt changes the space group to *Pccn*. In the anionic sublattice there is one Sb atom and four crystallographically independent Cl atoms. They form a deformed $[SbCl_6]^{3-}$ octahedron. We have used a similar numbering scheme to the anionic sublattice as in the high temperature phase to allow easier comparison of geometry. All atoms are in general positions. The bridging halogen atoms are ordered. The bond lengths around the antimony atom deviate more strongly from the ideal geometry than at 340 K, whereas the Cl-Sb-Cl valence angles are less distorted, due to the ordering of Cl1. Three *trans* Cl–Sb–Cl angles are between 173.9(1) and 178.4(1)° whereas the *cis* angles range from 85.45(6) to 94.77(6)°. As at 340 K, at 260 K there is observed a so-called *trans*-influence, which consists of a shortening of the Sb-Cl bonds placed opposite to those which are elongated by

N-H…Cl hydrogen bonds. The influence is mainly related to the stereochemical activity of the electron lone pair located on the Sb atom [12, 13].

In the asymmetric part of the unit cell there are two *n*-butylammonium cations. On lowering the temperature to T_{c1} the blocking of rotation of N1 cation takes place. As a result, $N1^{V}$-$H1A^{V}$…Cl2A hydrogen bonds are formed (Fig. 2c). The distance between $N1^{V}$ and Cl2A is changing from 3.496(10) Å at 340 K to 3.254(6) Å at 260 K ($\Delta = 0.242(10)$ Å). This has a very strong influence on the geometry of $SbCl_6^{3-}$ octahedron. The change in the position of the electron lone pair on the antimony atom leads to an increase of the Sb1-Cl2A bond length from 2.478(2) Å at 340 K to 2.575(2) Å at 260 K ($\Delta = 0.097(2)$ Å). The length of Sb1-$Cl1^{IV}$ decreases from 2.808(6) to 2.679(2) Å, whereas the length of $Sb1^{IV}$-$Cl1^{IV}$ increases from 2.928(5) at 340 K to 3.046(2) Å at 260 K ($\Delta = 0.118(5)$ Å) (Fig. 2c). The movement of the lone pair leads also to a shortening of the length of the Sb1-Cl2 bond from 2.478(2) Å at 340 K to 2.410(2) Å at 260 K.

The conformation of the N1 cation is typical for *n*-alkane chains. The torsion angles N1-C1-C2-C3 and C1-C2-C3-C4 amounts 173.8(15)° and −168.8(16)°, respectively. The N2 cation is still disordered (Fig. 3). The C7 atom is split between two positions with occupancy factors of 0.64 for C7 and 0.36 for C7A. The same type of disorder for the *n*-butylammonium cation was found in the structure of $(n\text{-}C_4H_9NH_3)_2[BiCl_5]$ [11]. It is suggested that the ethyl group of the alkylammonium chain undergoes a reorientation around the C5-C7 bond [11].

Structure at 100 K

In the low temperature phase (100.0(1) K) the crystal is orthorhombic, space group *Pccn*. There is no change in the space group on cooling from 260 K. The lowering of temperature leads to a freezing of reorientational motions of both cations. At 100 K both cations are ordered. The conformation of the N1 cation remains unchanged, whereas the N2 cation does not have *antiperiplanar* but *gauche* conformation (the dihedral angle N(2)-C(5)-C(6)-C(7) amounts to −70.4(9)°). This is in good agreement with the disorder observed at 260 K. There is an increased number of hydrogen bonds in the independent part of the unit cell. At 260 K there were two hydrogen bonds, whereas at 100 K there are six present (Table 4). The presence of a larger number of hydrogen bonds and their increased strength leads to a significant change of the coordination geometry of the antimony atom (see Fig. 2d).

Table 5. The calculated octahedral parameters Δ for $[SbCl_6]^{3-}$ octahedra for the $(C_4H_9NH_3)_2[SbCl_5]$ crystal at 340, 260 and 100 K.

Temperature [K]	Δ Parameter [$\cdot 10^3$]
340	5.87
260	6.98
100	7.82

On lowering temperature the Sb1-Cl4 bond length increases from 2.472(2) Å at 260 K to 2.527(2) Å at 100 K ($\Delta = 0.055(2)$ Å), whereas the opposite bond (Sb1–Cl3) is shortened from 2.877(2) Å at 260 K to 2.784(2) Å at 100 K ($\Delta = 0.093(2)$ Å). The reason for that is formation on cooling two hydrogen bonds (Fig. 2d); $N1^{VII}$-$H1B^{VII}$…Cl4 and $N2^{IV}$-$H2C^{IV}$…Cl3. The hydrogen bonds move the Sb^{III} lone pair in the Cl4 direction, resulting in a change of the geometry of the Sb1-Cl3 and Sb1-Cl4 bonds.

Formation of two new hydrogen bonds to Cl2A; N1-H1C…Cl2A and $N2^{VI}$-$H2B^{VI}$…Cl2A leads to the movement of the lone electron pair in the Cl2A direction (Fig. 2d). It results in changes in lengths of four Sb-Cl bonds. The Sb1-Cl2A bond length increases from 2.572(2) Å at 260 K to 2.733(2) Å at 100 K ($\Delta = 0.161(2)_{c1}$ Å), the $Cl1^{IV}$-Sb1 bond located opposite decreases its length from 2.679(2) to 2.533(2) Å ($\Delta = 0.146(2)$ Å). The changes in the next octahedron are much smaller. The $Sb1^{IV}$-$Cl1^{IV}$ bond increases its length from 3.046(2) Å at 260 K to 3.136(2) Å at 100 K ($\Delta = 0.090(2)$ Å), whereas the $Sb1^{IV}$-$Cl2^{IV}$ bond, which is lying opposite only slightly decreases its length ($\Delta = 0.010(2)$ Å) (Fig. 2d).

A measure of octahedral coordination distortion from regularity is provided by the distortion parameter for bond length [15] Δ:

$$\Delta = \frac{1}{6}\sum_{i+1}^{6}\left(\frac{R_i - \bar{R}}{\bar{R}}\right)^2$$

where $\bar{R}$ is the average Sb-Cl bond length within the octahedron and R_i the individual Sb-Cl bond length of the octahedron [16, 17].

The distortion parameters for the title structure at 340, 260 and 100 K (Table 5) clearly show that the $[SbCl_6]^{3-}$ octahedral geometry distortion increases on cooling, as expected. The same effect has been observed in other structures of chloroantimonates [15].

The changes in crystal geometry are due to thermal motions of the organic cations. These motions on decreasing temperature are consecutively frozen, what leads to the changes in the geometry of the anionic sublattice.

The anionic sublattice of the bismuth analogue (n-$C_4H_9NH_3)_2[BiCl_5]$ [6] is different. It is composed of isolated $Bi_2Cl_{10}^{4-}$ units, which are built of two $BiCl_6^{3-}$ octahedra sharing an edge. In the structure, there are two crystallographically independent n-butylammonium cations. They are connected to the anionic sublattice by N-H...Cl hydrogen bonds. At room temperature in the crystal lattice one of the cations is ordered, whereas the other one is disordered precisely in the same way as in (n-$C_4H_9NH_3)_2[SbCl_5]$ at 260 K. The bismuth analogue has one irreversible phase transition at *ca.* 370 K. On heating, above room temperature reorientational motions in the cationic sublattice are started, which lead to a breakdown of the crystal lattice before the melting point is reached. This leads to an increase in the freedom of the reorientational motions of the cations. The difference in behaviour between antimony and bismuth analogues is understandable, since the polyanionic $[\{SbCl_5\}^{2-}]_n$ sublattice makes the solid state more resistant to destruction.

Conclusions

Bis(n-butylammonium) pentachloroantimonate(III) undergoes two phase transitions at 229 and 315 K. Both are of the order-disorder type. At all temperatures the compound is orthorhombic. At 100 and 260 K the space group is *Pccn*, whereas at 340 K it is *Ibam*. The anionic sublattice is composed of distorted $[SbCl_6]^{3-}$ octahedra sharing two *cis* corners with two neighbouring entities, forming infinite one-dimensional $[\{SbCl_5\}^{2-}]_n$ chains. The distortions of the anionic sublattice are related to the type of the polyanionic substructure and the presence and strength of the N–H...Cl hydrogen bonds. The mechanism of the phase transition at 315 K is related to the ordering on cooling of one out of two independent n-butylammonium cations located on a special position. The second phase transition at 229 K is taking place without change of the space group. Ordering of cations on lowering temperature takes place by freezing their reorientational motions. It leads to the formation of N-H...Cl hydrogen bonds, which results in significant deformation of the anionic sublattice.

Experimental Section

The title compound was obtained by mixing n-butylammonium chloride and antimony trichloride (molar ratio from 2 : 1), in an aqueous solution of hydrochloric acid. Single crystals suitable for X-ray diffraction analysis were grown by slow evaporation of the solvent at r. t. X-ray measurements were performed on Xcalibur single crystal diffractometer equipped with an Oxford Cryosystems cooler. The *ω-scan* technique was used. For all data Lorentz, polarisation and semiempirical absorption corrections based on symmetry equivalent reflections [18] were performed ($T_{min} = 0.143$, $T_{max} = 0.108$ at 100 K, $T_{min} = 0.145$, $T_{max} = 0.108$ for the structure at 260 K and $T_{min} = 0.148$, $T_{max} = 0.106$ at 340 K).

All structures were solved by the Patterson method. For all non-hydrogen atoms anisotropic displacement parameters were refined. The positions of the hydrogen atoms were refined using a riding model. The hydrogen atoms were added to all C and N atoms for the 100 K and 260 K cases, and to the N atoms only in the case of the disordered cations at 340 K. The details of data collection and refinement are listed in Table 1.

The quantity minimised was $\Sigma w([|F_o - F_c)^2$ with the weighting scheme $w_1 = 1/[\sigma^2(F_o{}^2) + 40.6409P]$, $w_2 = 1/[\sigma^2(F_o{}^2) + (0.0407P)^2]$ and $w_3 = 1/[\sigma^2(F_o{}^2) + (0.0753P)^2 + 1.0077P]$, where $P = (F_o{}^2 + 2F_c{}^2)/3$ at 100, 260 and 340 K, respectively.

The Oxford diffraction software CrysAlisCCD and CrysAlisRED programs were used during the data collection, cell refinement and data reduction processes [18]. The SHELX-97 [19] and SHELXTL [20] programs were used for structure solutions, refinements and structure drawings.

Crystallographic data (excluding structure factors) for (n-$C_4H_9NH_3)_2SbCl_5$ at 100 K, 260 K and 340 K have been deposited at the Cambridge Crystallographic Data Centre as supplementary publication nos. CCDC 296781 - 296783. Copies of data may be obtained free of charge, on application to the Director, CCDC, 12 Union Road, Cambridge CB2 1EZ, UK (Fax: int. code+(1223) or e-mail: data_request@ccdc.cam.ac.uk).

Acknowledgement

Bartosz Zarychta is a holder of a scholarship (Domestic Grant for Young Scientists) of the Foundation for Polish Science in 2006.

[1] R. Jakubas, L. Sobczyk, Phase Trans. **20**, 163 (1990).
[2] L. Sobczyk, R. Jakubas, J. Zaleski, Polish J. Chem. **71**, 265 (1997).
[3] J. Jóźków, R. Jakubas, G. Bator, A. Pietraszko, J. Chem. Phys, **114**, 7239 (2001).
[4] J. Zaleski, A. Pietraszko, Acta Crystallogr. **B52**, 287 (1996).
[5] N. Piślewski, J. Tritt-Goc, R. Jakubas, Phys. Status Solidi **193B**, 67 (1996).
[6] P. Ciąpała, R. Jakubas, G. Bator, J. Zaleski, A. Pietraszko, M. Drozd, J. Baran, J. Phys.: Condens. Matter **9**, 627 (1997).
[7] J. Zaleski, Structure, Phase Transitions and Molecular Motions in Chloroantimonates(III) and -Bismuthates(III). Opole University Press, Opole, Poland (1995).
[8] T. Okuda, Y. Kinoshita, H. Terao, K. Yamada, Z. Naturforsch. **49a**, 185 (1993).
[9] R. Jakubas, P. Ciąpała, G. Bator, Z. Ciunik, R. Decressain, J. Refebvre, J. Baran, Physica **B217**, 67 (1996).
[10] K. Prasides, P. Day, A. K. Cheetham, Inorg. Chem. **24**, 545 (1985).
[11] P. Szklarz, J. Zaleski, R. Jakubas, G. Bator, W. Medycki, K. Falińska, J. Phys. Condens. Matter **17**, 2509 (2005).
[12] R. J. Gillespie, Chem. Soc. Rev. **21(1)**, 59 (1992).
[13] X. Wang, F. Liebau, Acta Crystallogr. **B52**, 7 (1996).
[14] J. Zaleski, A. Pietraszko, J. Mol. Struct. **327**, 287 (1994).
[15] M. Bujak, R. J. Angel, J. Solid State Chemistry **178**, 2237 (2005).
[16] K. Robinson, G. V. Gibbs, P. H. Ribbe, Science **172**, 567 (1971).
[17] I. D. Brown, R. H. Shannon, Acta Crystallogr. **A29**, 266 (1978).
[18] Oxford Diffraction; CrysAlis CCD, Data collection GUI for CCD and CrysAlis RED, CCD data reduction GUI versions 1.169.5 and 1.170.16, Oxford Diffraction Poland (2002).
[19] G. M. Sheldrick, SHELX-97. Program for the Solution and the Refinement of Crystal Structures. University of Göttingen, Germany (1997).
[20] G. M. Sheldrick, SHELXTL. Siemens Analytical X-ray Instrument Inc., Madison, Winsconsin, USA (1990).